

USI Technical Report Series in Informatics

Evaluating realistic tsunami simulations with SWE model on GPU-enabled clusters

Juraj Kardos¹

¹ Faculty of Informatics, Università della Svizzera italiana, Switzerland

Abstract

Tsunamis are devastating natural disasters, potentially able to create a lot of damage. In order to predict such events and their behavior fast and detailed simulations of tsunamis are required. In this paper we evaluate the ability of SWE shallow water numerical model to perform efficient and realistic tsunami simulations. We used SWE model to reproduce 2004 Great Sumatra–Andaman and 2011 Tōhoku tsunami.

Nowadays, many of the Top500 supercomputers are using GPU accelerators to enhance the peak performance. The GPU-enabled clusters Tesla-CMC and Todi Cray XK-7 were benchmarked using different number of processes and GPUs to obtain the most efficient and the most fast SWE configurations. Using all 3 available GPUs of Tesla-CMC, we observed the maximum speedup of 158x in comparison to single-core CPU version. The most efficient configuration was the one with a single GPU, achieving speedup of 58x. Performance results for “Todi” Cray XK-7 are also presented for larger number of compute nodes.

Report Info

Published
July 2013

Number
USI-INF-TR-2013-3

Institution
Faculty of Informatics
Università della Svizzera italiana
Lugano, Switzerland

Online Access
www.inf.usi.ch/techreports

1 Introduction

Tsunamis belong to the most devastating ocean disasters in the world. When they reach the dense-populated coastline areas unexpectedly, fatal destructions and lot of deads are claimed. In order to prevent such scenarios, it is required to have a tool that would provide fast and detailed simulation of tsunami. One of the models that could be used for tsunami simulation is SWE model [4, 1].

Tsunamis are massive oceanic waves generated by underwater earthquakes. The earthquakes are caused by collision of multiple tectonic plates. During such events plates are usually slipped over each other or deformed in that way they cause the displacement of the sea floor and increase of the water level. The resulting tsunami propagates into all directions from the source region by gravitational force. This study deals with Sumatra 2004 and Tōhoku 2011 tsunamis.

Shallow water equations [5] (the underlying mathematical concept of the SWE model) describe the behavior of a fluid, in particular water, in a two-dimensional domain. The main modeling assumption of the equations is that we can neglect effects of flow in vertical direction. This conditions holds if we think of ocean in global terms, i.e., horizontal lengths are much greater than vertical lengths (the ocean depth). Shallow water equations describe the change of water depth h and horizontal velocities v_x and v_y over time, depending on some initial conditions, in this case – ocean floor displacement during the earthquake. The respective changes of water depth h in time can be described by a system of partial differential equations (1).

High-resolution tsunami simulations result into large problems, that could often be solved in reasonable time only using parallel computations. This study is aimed to find the most efficient configuration and evaluate performance of emerging massively-parallel graphics processing units (GPUs).

The paper is organized as follows. Section 2 provides description of used data and earthquake model. It describes their meaning, origin, transformations and how the data were used in order to obtain the result. Section 3 provides experimental results and analyses the credibility of performed simulations. Speedup and parallel efficiency of different SWE configurations are discussed in Section 4.

$$\begin{cases} \frac{\partial h}{\partial t} + \frac{\partial(v_x h)}{\partial x} + \frac{\partial(v_y h)}{\partial y} = 0, \\ \frac{\partial(hv_x)}{\partial t} + \frac{\partial(hv_x v_x)}{\partial x} + \frac{\partial(hv_y v_x)}{\partial y} + \frac{1}{2}g \frac{\partial(h^2)}{\partial x} = -gh \frac{\partial b}{\partial x}, \\ \frac{\partial(hv_y)}{\partial t} + \frac{\partial(hv_x v_y)}{\partial x} + \frac{\partial(hv_y v_y)}{\partial y} + \frac{1}{2}g \frac{\partial(h^2)}{\partial y} = -gh \frac{\partial b}{\partial y}, \\ h|_{t=0}(x, y) = h_0(x, y). \end{cases} \quad (1)$$

2 Simulation methodology

The basic flow of the simulation pipeline is shown in the Figure 1. The skewed rectangles represent data files and the regular rectangles with double vertical borders represent applications and tools.

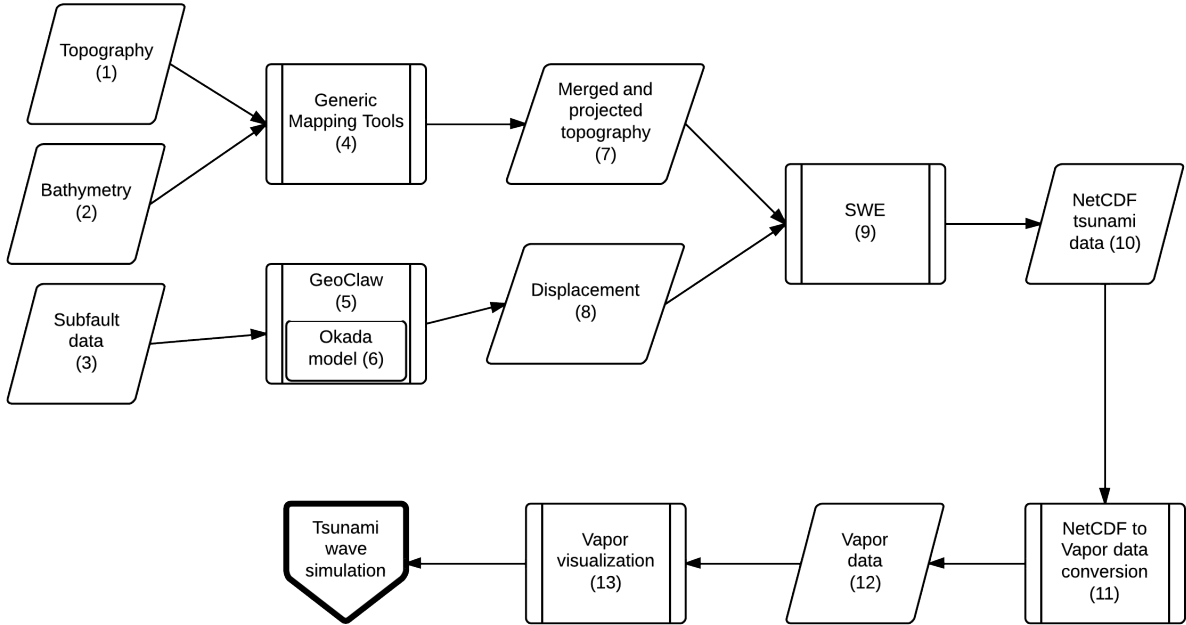


Figure 1: Simulation methodology flowchart of components

2.1 Input files and preprocessing

In the SWE model tsunami is identified by the number of input data fields. First of all, we need the model of the Earth's surface including the mainland as well as the ocean floor (items (1) and (2) in Figure 1). ETOPO1 [3] Global Relief Model is a 1 arc-minute (~1.8 km) model of Earth's surface that integrates land topography and ocean bathymetry. The global 30 arc-second grid (~0.9 km) ocean floor relief (bathymetry) is provided by GEBCO [2].

The relief data cannot be used by the SWE in the raw form. The basic data structure of the SWE is a rectangular plain grid. The bathymetry (2) and topography (1) data need to be projected on the grid (7) including the whole region of interest. For this purpose Generic Mapping Tools (4) are used. GMT merge topography and bathymetry data and generate the rectangular grid of region (7) defined by latitude and longitude coordinates.

We also need a model of the seismic event that triggered the tsunami. The tsunami is initiated when the sea floor displacement occurs. We need to know several aspects of the event including the exact area of

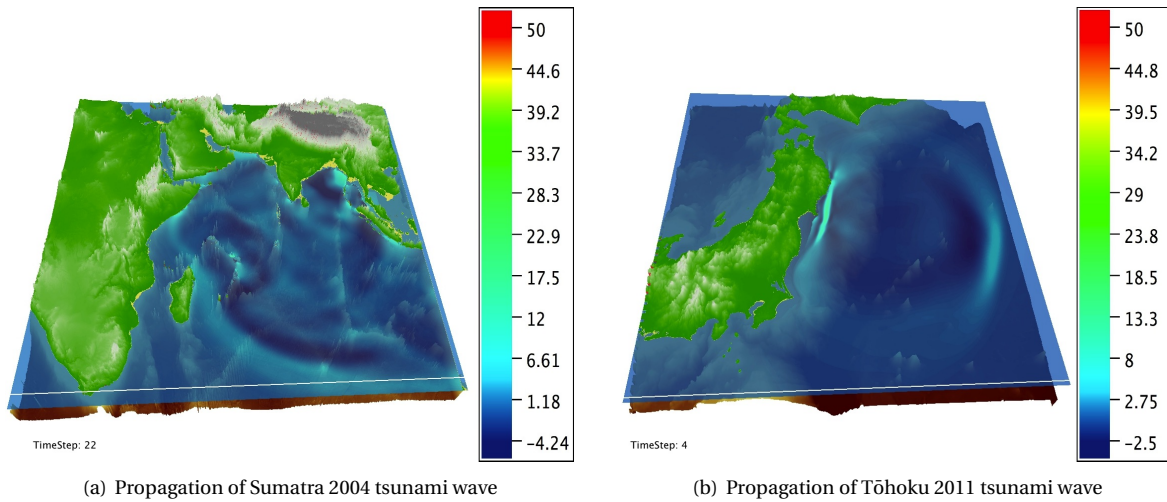


Figure 2: Visualization of tsunami waves

the sea floor that was displaced, how much it was displaced and the time and direction of the movement. The movement of the sea floor is estimated using various sensor measurements in the area affected by the earthquake. These measurements are usually maintained by U.S. Geological Survey, which also provides the data in several formats. The SWE is configured for the subfault format (3).

In case of the tsunami simulation we are not interested in the seismic activity itself. We only need to know the initial displacement of the sea floor, i.e. the initial state of the tsunami wave. The resulting wave propagation can be computed with SWE model. To get the displacement (8) we need to transform the subfault data (3). This transformation is defined in the Okada model (6) [8], which is analytical model for computing displacement from subfault and is a part of GeoClaw pack (5) [6]. It predicts surface displacement according to a specified rectangular dislocation at depth using Green's functions. According to [12], Okada model may be sufficient for simulating large intra-continental earthquakes but it has limitations in simulating small area earthquakes.

2.2 Postprocessing and visualization

The result of simulation is encoded in NetCDF format (10). The NetCDF encodes data in the self-describing and machine independent manner. When SWE used in parallel mode a separate NetCDF file is created for each MPI process. We visualize the simulation output with VAPOR, which eases the process by compressing the huge amount of original NetCDF data, yet conserving most of the important detail. The conversion step (11) could be done on server resulting into much smaller file to be transferred and visualized on user machine (12-13).

3 Experimental results

The Great Sumatra–Andaman earthquake of December 26th, 2004 occurred on the interface of the India and Burma plates and was caused by the release of stresses that develop as the India plate subducts beneath the overriding Burma plate. An estimated 1,600 kilometers of fault surface slipped about 15 meters along the subduction zone where the Indian Plate slides under the overriding Burma Plate. The sudden vertical rise of the seabed during the earthquake displaced massive volumes of water, resulting in a tsunami that struck the coasts of the Indian Ocean. The tsunami was noticed as far as Struisbaai in South Africa, 8,500 km away, where a 1.5 m high tide surged on shore about 16 hours after the earthquake [10].

In case of great Sumatra–Andaman earthquake and tsunami the rupture process was estimated using tsunami waveforms observed at tide gauges and the coseismic vertical deformation observed along the coast [11]. The tsunami waveform inversion was used to estimate the slip distribution of the earthquake. The fault area of the earthquake is divided into several smaller subfaults and the slip amount on each subfault is estimated from the observed tsunami waveforms.

The magnitude 9.0 Tohoku earthquake on March 11, 2011, which occurred near the northeast coast of Honshu, Japan, resulted from thrust faulting on or near the subduction zone plate boundary between the Pacific and North America plates. Modeling of the rupture of this earthquake indicate that the fault moved upwards of 30-40 m, and slipped over an area approximately 300 km long (along-strike) by 150 km wide (in the down-dip direction) [9]. The tsunami propagated throughout the Pacific Ocean region reaching the entire Pacific coast of North and South America from Alaska to Chile. Tsunami around the coastline of Japan reached heights from 3 to 6 m.

Simulation of the tsunami wave propagation can begin after the initial sea floor displacement (7) and initial waveform have been computed. Propagation model and the behavior of the wave is defined in the SWE model. Wave propagation is simulated for specified time range and on specific area of interest defined relative to the epicenter. SWE is able to adapt time step for numerical stability conditions. Visualization of wave propagation can be seen in Figure 2.

SWE can be configured to run in parallel or to use GPU accelerators in order to speed up the simulation. Detailed description of used configurations and the resulting speed up and efficiency is discussed in the section 4.

3.1 Credibility of performed tsunami simulations

Credibility of the performed tsunami simulations has been verified by comparison to numerous reports containing the list of mainland areas hit by tsunami, observations of the tsunami wave and ocean level sensors measurements.

The great Sumatra–Andaman tsunami has been observed in 14 countries in South Asia and East Africa. The tsunami caused more casualties than any other in recorded history and was recorded nearly world-wide on tide gauges in the Indian, Pacific and Atlantic Oceans. Seiches were observed in India and the United States. Subsidence and landslides were observed in Sumatra [10]. According to our SWE results, the tsunami wave reveals the propagation through the whole Indian Ocean and shows the wave hitting the adjacent coastline areas. Wave continues to propagate through the open ocean reaching the coastline of Africa. On its arrival on shore, the height of the tsunami varied greatly, depending on its distance and direction from the epicentre and other factors such as the local bathymetry. Reports have the height ranging from 2-3 m at the African coast near Kenya [7]. Simulation revealed the height of tsunami waves reaching the Kenyan coastline of approximately the same height. The tsunami was observed also in Struisbaai, South Africa, where a 1.5 m high tide surged on shore [10]. Similar results were observed in the simulation.

In the case of Tōhoku, the majority of casualties and damage occurred in Iwate, Miyagi and Fukushima from a Pacific-wide tsunami with a maximum runup height of 37.88 m at Miyako. The tsunami destroyed or severely damaged many coastal towns in the Kuji-Minamisanriku-Nami area [9]. According to our SWE results, tsunami was spreading in the direction of the most affected islands of Honshu and Hokkaido but the wave was eliminated just before reaching the coastline areas. This behavior is probably caused by some numerical constraints in the SWE model.

4 Benchmarking

The SWE has been run with different configurations to find out the most efficient settings. SWE was used in parallel mode with 1 to 8 MPI processes and also with GPUs included. The simulations were run on two different clusters: Tesla-CMC, equipped with NVIDIA Tesla C2075 GPUs and Todi Cray XK-7, equipped with NVIDIA K20 GPUs. The summarization of the speedups can be found in the Table 1, 2 and 3; Table 4 presents the efficiency of different configurations.

It is obvious from results that when higher degree of parallelism is used the speedup is increased but the efficiency is decreasing because of the inter-process communication. When the GPU is used the speedup increases dramatically. When multiple GPUs are used, speedup continues to increase, while the efficiency only slightly decreases.

5 Conclusion

In this paper we presented the realistic tsunami simulations with an emphasis on how fast and detailed solution could be achieved on emerging parallel architectures. Such simulations are important for analysis and prediction of catastrophic scenarios in dense-populated areas reachable by tsunamis.

The propagation of the tsunami wave is computed using the SWE water wave propagation model. The SWE model works with subfault earthquake model from which is computed initial sea floor displacement using Okada transformation. Several data files with representation of ocean bathymetry and mainland topography are needed for the simulation. Great Sumatra–Andaman tsunami of 2004 and Tōhoku 2011 tsunami simulations have been performed.

The SWE model has been run with different configurations to benchmark the performance of the GPU-enabled clusters Tesla-CMC and Todi Cray XK-7. SWE model has been run in parallel mode with multiple CPU processes with and without using GPUs. The performance of the massively-parallel graphics processing units (GPUs) have shown impressive results. Using all available GPUs, we observed the maximum speedup of 158x in comparison to single-core CPU version. The most efficient configuration was the one with a single GPU, achieving speedup of 58x.

I would like to thank Dmitry Mikushin of the University of Lugano, Sebastian Rettenberger and Alexander Breuer of SWE model development team for their help with the various technical issues. Imagery produced by VAPOR (www.vapor.ucar.edu), a product of the Computational Information Systems Laboratory at the National Center for Atmospheric Research. This study has been performed as a part of “Parallel & Distributed Computing Lab” course in the University of Lugano.

References

- [1] Alexander Breuer and Michael Bader. Teaching parallel programming models on a shallow-water code. In *ISPDC*, pages 301–308. IEEE Computer Society, 2012.
- [2] British Oceanographic Data Center. General bathymetric chart of the oceans. https://www.bodc.ac.uk/data/online_delivery/gebco/.
- [3] National Geophysical Data Center. Global relief model. <http://www.ngdc.noaa.gov/mgg/global/>.
- [4] Michael Bader et al. SWE – the Shallow Water Equations teaching code. <https://github.com/TUM-I5/SWE>, Jun 2012.
- [5] R. W. Hamming. *Numerical Methods for Scientists and Engineers*. Dover, 1986.
- [6] R. J. LeVeque and M. J. Berger et al. Clawpack software. www.clawpack.org.
- [7] Bureau of Meteorology. Tsunami facts and information. <http://www.bom.gov.au/tsunami/info/>.
- [8] Yoshimitsu Okada. Surface deformation due to shear and tensile faults in a half-space. *Bull Seismol Soc Am*, 75:1135–1154, 1985.
- [9] U.S. Geological Survey. Magnitude 9.0 - near the east coast of Honshu. <http://earthquake.usgs.gov/earthquakes/eqinthenews/2011/usc0001xgp/>.
- [10] U.S. Geological Survey. Magnitude 9.1 - off the west coast of Northern Sumatra. <http://earthquake.usgs.gov/earthquakes/eqinthenews/2004/us2004slav/>.
- [11] Y. Tanioka and T. Kususe et al. Rupture process of the 2004 Great Sumatra-Andaman earthquake estimated from tsunami waveforms. *Earth Planets Space*, 58:203–209, 2006.
- [12] Chisheng Wang and Xinjian Shan et al. Using finite element and okada models to invert coseismic slip of the 2008 mw 7.2 yutian earthquake, china, from insar data. *J Seismol*, 17:347D360, 2013.

Config \ Process	0	1	2	3	4	5	6	7
MPI-1	1.00	-	-	-	-	-	-	-
MPI-2	1.75	1.75	-	-	-	-	-	-
MPI-3	2.60	2.60	2.60	-	-	-	-	-
MPI-4	3.46	3.46	3.46	3.46	-	-	-	-
MPI-5	4.12	4.12	4.12	4.12	4.12	-	-	-
MPI-6	4.91	4.91	4.91	4.91	4.91	4.91	-	-
MPI-7	5.59	5.59	5.59	5.59	5.59	5.59	5.59	-
MPI-8	6.30	6.30	6.30	6.30	6.30	6.30	6.30	6.30
MPI-GPU-1	55.33	-	-	-	-	-	-	-
MPI-GPU-2	106.60	106.73	-	-	-	-	-	-
MPI-GPU-3	155.06	157.29	158.10	-	-	-	-	-

Table 1: Performance of Tohoku tsunami simulation on *Tesla-CMC*, speedups relative to single CPU time (36,034 sec)

Config \ Process	0	1	2	3	4	5	6	7
MPI-1	1.00	-	-	-	-	-	-	-
MPI-2	1.90	1.90	-	-	-	-	-	-
MPI-3	2.76	2.76	2.76	-	-	-	-	-
MPI-4	3.74	3.74	3.74	3.74	-	-	-	-
MPI-5	4.50	4.50	4.50	4.50	4.50	-	-	-
MPI-6	5.29	5.28	5.29	5.29	5.29	5.29	-	-
MPI-7	6.15	6.16	6.16	6.18	6.16	6.17	6.15	-
MPI-8	6.91	6.91	6.91	6.91	6.91	6.91	6.91	6.91
MPI-GPU-1	58.32	-	-	-	-	-	-	-
MPI-GPU-2	105.88	107.18	-	-	-	-	-	-
MPI-GPU-3	147.16	151.74	153.40	-	-	-	-	-

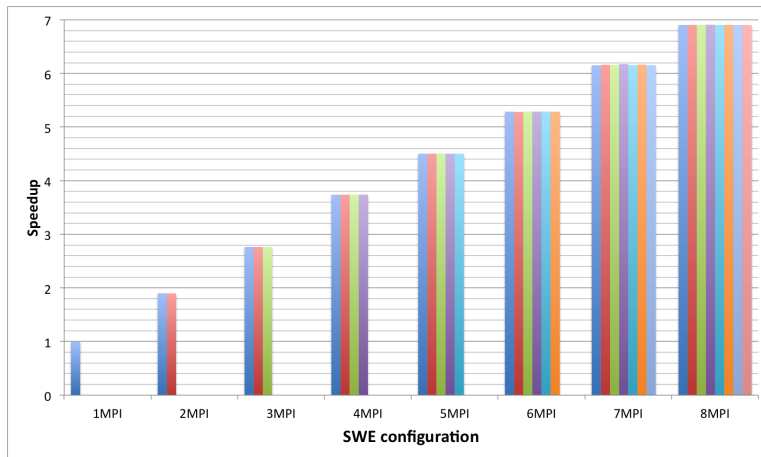
Table 2: Performance of Sumatra tsunami simulation on *Tesla-CMC*, speedups relative to single CPU time (16,954 sec)

Config \ Process	0	1	2	3	4	5	...	16	32	48	64
MPI-16	1.00	1.00	1.00	1.00	1.00	1.01	...	1.00	-	-	-
MPI-32	1.94	1.94	1.94	1.94	1.94	1.94	...	1.94	1.94	-	-
MPI-48	2.90	2.90	2.90	2.90	2.89	2.90	...	2.90	2.90	2.89	-
MPI-64	3.88	3.88	3.88	3.88	3.88	3.88	...	3.88	3.88	3.88	3.88
MPI-GPU-1	14.43	-	-	-	-	-	...	-	-	-	-
MPI-GPU-2	29.22	29.08	-	-	-	-	...	-	-	-	-
MPI-GPU-4	61.35	60.99	61.06	60.64	-	-	...	-	-	-	-
MPI-GPU-8	116.16	111.05	109.83	113.49	110.14	110.62	...	-	-	-	-
MPI-GPU-16	103.03	82.23	103.12	97.98	103.69	102.11	...	104.14	-	-	-
MPI-GPU-32	260.99	225.87	237.98	248.89	264.56	259.76	...	235.67	251.78	-	-

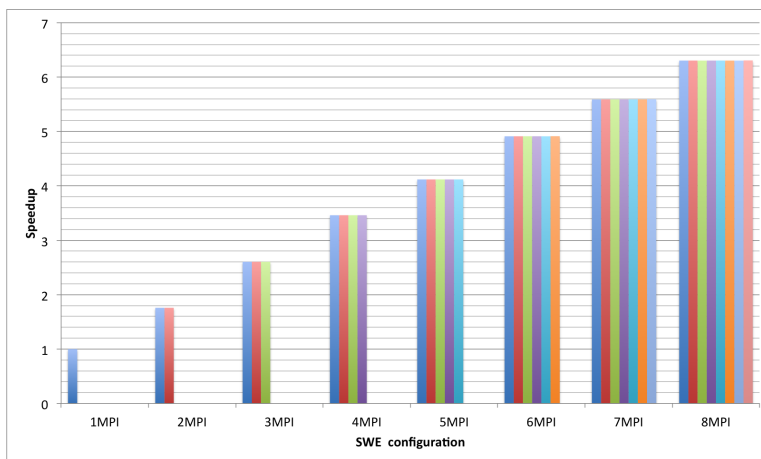
Table 3: Performance of Tohoku tsunami simulation on *Todi Cray XK-7*, speedups relative to process 0 time with usage of one full node (6,027.5 sec)

Config	Sumatra 2004	Tohoku 2011
MPI-1	1.000	1.000
MPI-2	0.950	0.879
MPI-3	0.921	0.868
MPI-4	0.935	0.865
MPI-5	0.900	0.824
MPI-6	0.881	0.819
MPI-7	0.880	0.799
MPI-8	0.863	0.789
MPI-GPU-1	58.322	55.331
MPI-GPU-2	53.263	53.332
MPI-GPU-3	50.241	52.269

Table 4: Parallel efficiency of tsunami simulation on *Tesla-CMC*



(a) Sumatra tsunami simulation



(b) Tohoku tsunami simulation

Figure 3: Observed speedups with different number of CPU processes on *Tesla-CMC*

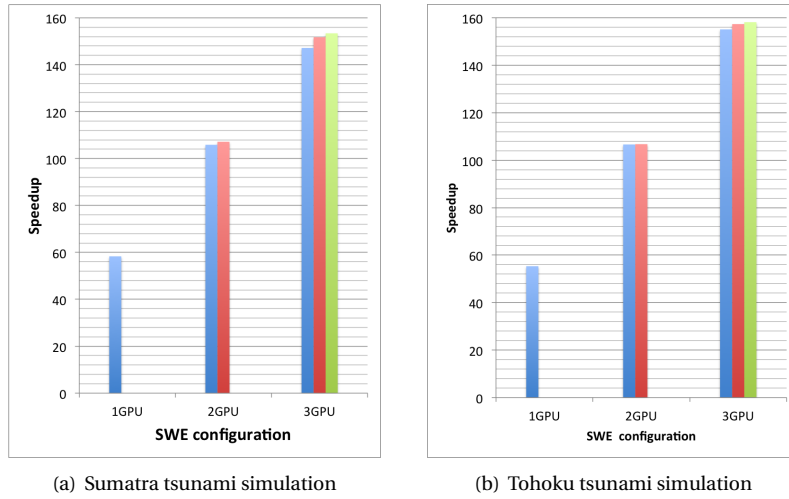
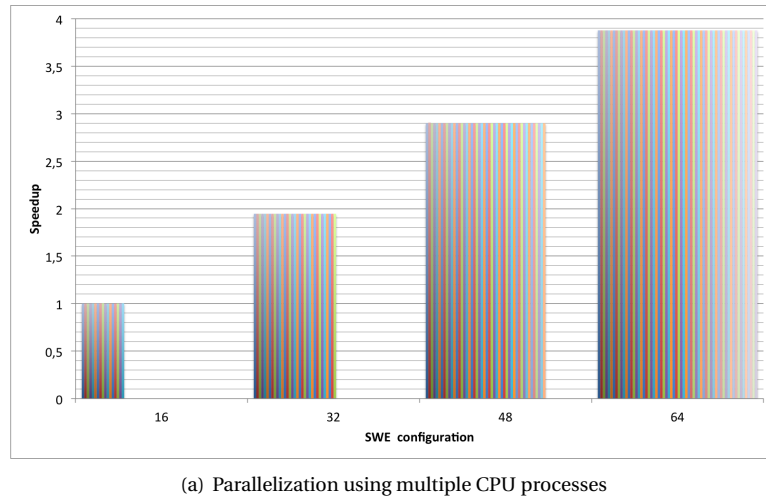
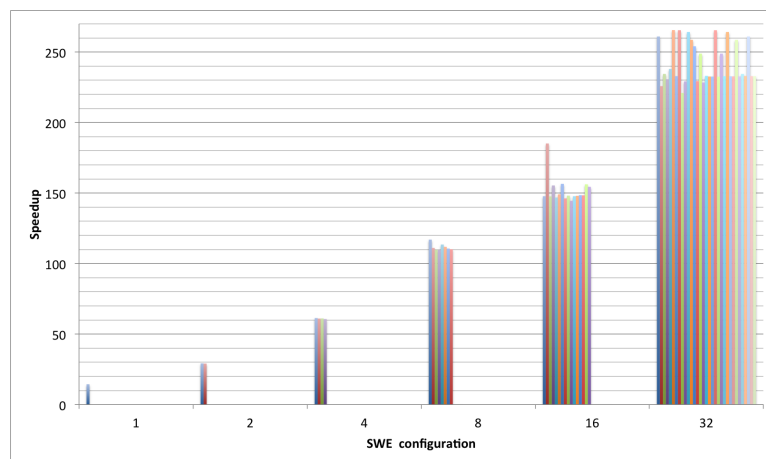


Figure 4: Observed speedups with different number of GPUs on *Tesla-CMC*



(a) Parallelization using multiple CPU processes



(b) Parallelization using multiple CPU processes with GPUs

Figure 5: Observed speedups with different configurations on *Todi Cray XK-7*